High-pressure x-ray tomography microscope: Synchrotron computed microtomography at high pressure and temperature

Yanbin Wang[a] and Takeyuki Uchida
GeoSoilEnviroCARS, Center for Advanced Radiation Sources, The University of Chicago, 5640 S. Ellis Avenue, Chicago, Illinois 60637

Frank Westferro
ChemMatCARS, Center for Advanced Radiation Sources, The University of Chicago, 5640 S. Ellis Avenue, Chicago, Illinois 60637

Mark L. Rivers and Norimasa Nishiyama
GeoSoilEnviroCARS, Center for Advanced Radiation Sources, The University of Chicago, 5640 S. Ellis Avenue, Chicago, Illinois 60637

Jeff Gebhardt
ChemMatCARS, Center for Advanced Radiation Sources, The University of Chicago, 5640 S. Ellis Avenue, Chicago, Illinois 60637

Charles E. Lesher
Department of Geology, University of California at Davis, Davis, California 95616

Steve R. Sutton
GeoSoilEnviroCARS, Center for Advanced Radiation Sources, The University of Chicago, 5640 S. Ellis Avenue, Chicago, Illinois 60637

(Received 3 May 2005; accepted 29 May 2005; published online 12 July 2005)

A new apparatus has been developed for microtomography studies under high pressure. The pressure generation mechanism is based on the concept of the widely used Drickamer anvil apparatus, with two opposed anvils compressed inside a containment ring. Modifications are made with thin aluminum alloy containment rings to allow transmission of x rays. Pressures up to 8 GPa have been generated with a hydraulic load of 25 T. The modified Drickamer cell is supported by thrust bearings so that the entire pressure cell can be rotated under load. Spatial resolution of the high pressure tomography apparatus has been evaluated using a sample containing vitreous carbon spheres embedded in FeS matrix, with diameters ranging from 0.01 to 0.2 mm. Spheres with diameters as small as 0.02 mm were well resolved, with measured surface-to-volume ratios approaching theoretical values. The sample was then subject to a large shear strain field by twisting the top and bottom Drickamer anvils. Imaging analysis showed that detailed microstructure evolution information can be obtained at various steps of the shear deformation, allowing strain partition determination between the matrix and the inclusions. A sample containing a vitreous Mg_2SiO_4 sphere in FeS matrix was compressed to 5 GPa, in order to evaluate the feasibility of volume measurement by microtomography. The results demonstrated that quantitative inclusion volume information can be obtained, permitting *in situ* determination of *P-V-T* equation of state for noncrystalline materials. © *2005 American Institute of Physics.* [DOI: 10.1063/1.1979477]

I. INTRODUCTION

X-ray computed tomography (CT) is a well-known method for reconstructing three-dimensional images of a structure from a finite number of radiographic images. Since the development of synchrotron sources, advanced CT systems have been developed to approach spatial resolutions to about 1 μm, sufficient to begin effective microstructure imaging in three dimensions.[1,2] These high-resolution techniques are sometimes called x-ray tomographic microscopy (XTM) to emphasize the distinction between three-dimensional (3D) microtomography and what is microscopic imaging (2D).[3,4] The most important advantage of XTM over serial sectioning methods is that tomographic methods are nondestructive. This means that the same sample can be characterized many times. It is possible to characterize samples *in situ*, *in vitro*, and in some cases, *in vivo* and observe how microstructures evolve in response to processing, degradative environments, or mechanical loading.

However, there has been no systematic effort in performing high pressure XTM (HPXTM), largely due to the fact that it is difficult to conduct tomographic imaging under pressure. In this article, we describe a new apparatus for XTM studies under simultaneous high pressure and temperature. The new apparatus will not only enable us to study

[a]Author to whom correspondence should be addressed; electronic mail: wang@cars.uchicago.edu

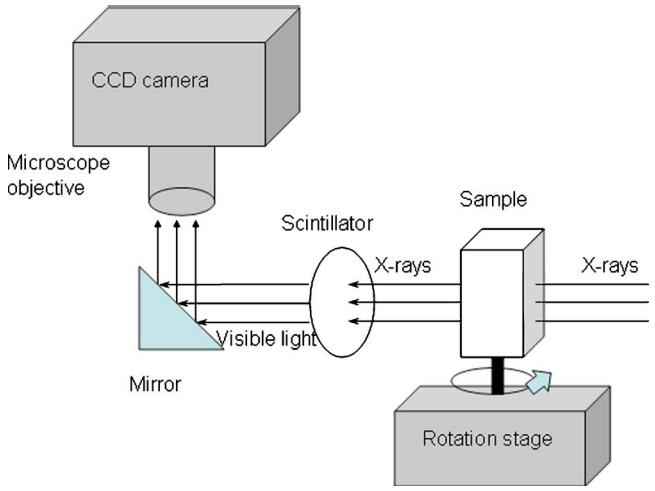

FIG. 1. (Color online) Conceptual diagram illustrating the principles of a typical conventional microtomography setup.

microstructural evolution of materials under high pressure, but also has several important additional applications, which will be discussed.

II. SYSTEM DESIGN CONCEPT

A. A brief description of microtomography

X-ray computed microtomography (CMT) is similar to a medical computed axial tomography (CAT) scan where x-ray images are taken at many angles around the object and virtual slices through the object are reconstructed.[6] A schematic of the conventional CMT apparatus is shown Fig. 1. The sample is rotated, with the axis of rotation perpendicular to the plane of the incident beam, by a discrete angular interval determined by the linear resolution desired. The transmission of each ray through the sample, along a line from the source to the detector, represents a line integral of the attenuation coefficients along this ray. The procedure is repeated for each angular view until the sample has been rotated by 180° in the x-ray beam. The transmitted x-ray intensities recorded in the detector, obtained for each view in the slice, are then processed using a filtered back-projection algorithm to reconstruct the horizontal slice. A 3D reconstruction with spatial resolution of 1 μm has been achieved.[7] Furthermore, the intensity variations in the images contain information on elemental composition variations inside the sample, if the overall bulk composition is known.

B. Design criteria—general considerations

In order to conduct CMT under pressure, a special high pressure apparatus must be constructed. The following requirements are considered for the design of high-pressure tomography apparatus: (1) it must be able to generate enough pressure—our goal is 10 GPa; (2) the sample under high pressure must be able to be accurately rotated so that tomography images can be collected; (3) the sample chamber must be transparent to the x rays to allow absorption contrast to be recorded; and (4) the sample should be large enough in order to obtain information on microstructure and its evolution in a meaningful way. In addition, we require (5) that the apparatus must be small enough to fit into the existing 250 ton hydraulic press at beamline 13-BM-D of the Advanced Photon Source;[8] and (6) the ability to rotate the two opposing Drickamer anvils in opposite directions under high pressure, to generate large shear strains in the sample for deformation studies.

These criteria can be met with a basic design concept inspired by the rotational deformation apparatus (RDA),[5] where a Drickamer cell is used to generate pressure (some details of the Drickamer anvil apparatus is given in the next section). A modification of the RDA rotation mechanism results in a flexible apparatus, which can be used both as a RDA and a high pressure tomography apparatus, described in the following sections.

C. Special imaging requirements

In order to perform tomography imaging through the pressure vessel, high photon energies are needed. In addition, large monochromatic x-ray beams are required to cover the entire sample. In order to remove artifacts such as imperfections in the optics (nonuniformities in the x-ray beam intensity or yttrium-aluminum-garnet (YAG) scintillator), it is a common practice to collect white field images by driving the sample completely out of the beam path. By dividing the intensity for each sample image by this white field, effects of virtually all instrument imperfections can be removed. In our case, however, it is not ideal to collect white field images through open air because harmonic contents of the monochromatic beam are different with and without the absorbing apparatus. One way to circumvent this problem is to collect reference background images through the containment ring. In order to do this, however, the ring material must be homogeneous enough to minimize unwanted intensity variations.

III. THE HIGH-PRESSURE X-RAY TOMOGRAPHIC MICROSCOPE

A. The x-ray transparent rotational Drickamer cell

The Drickamer cell is a well known and widely used device for high-pressure experimentation (Fig. 2). It is an opposed anvil device, similar to the Bridgman anvil apparatus and the diamond anvil cell (DAC). However, the anvils are compressed inside a containment ring, which restricts the extrusion of the pressure media. This feature of the Drickamer cell helps to maintain sample geometry, unlike the Bridgman device or the DAC where the sample is extruded laterally under high pressure, reducing its usefulness for microtomography studies.

The traditional Drickamer cell uses a thick containment ring, made of either hardened steel or tungsten carbide, both of which are x-ray opaque. This is not suitable for microtomography experiments, as the entire sample along with the pressure medium needs to be imaged. Our solution is to replace the containment ring with a thin and light Al alloy ring, which allows modest pressure generation and is transparent to x rays (Fig. 2). Al alloy is readily available, inexpensive, and homogeneous in physical properties. The dimensions of the Al containment ring, the tapering angle of the Drickamer

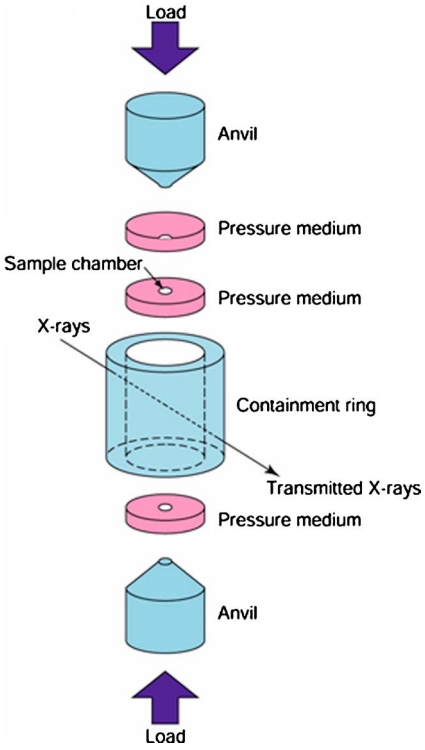

FIG. 2. (Color online) The Drickamer anvil cell. WC anvils are used in our experiments, with various tapering angles and truncation tip size. The pressure medium is a mixture of amorphous boron and epoxy resin. The containment ring is made of an Al alloy, with wall thicknesses varying from 5 to 10 mm.

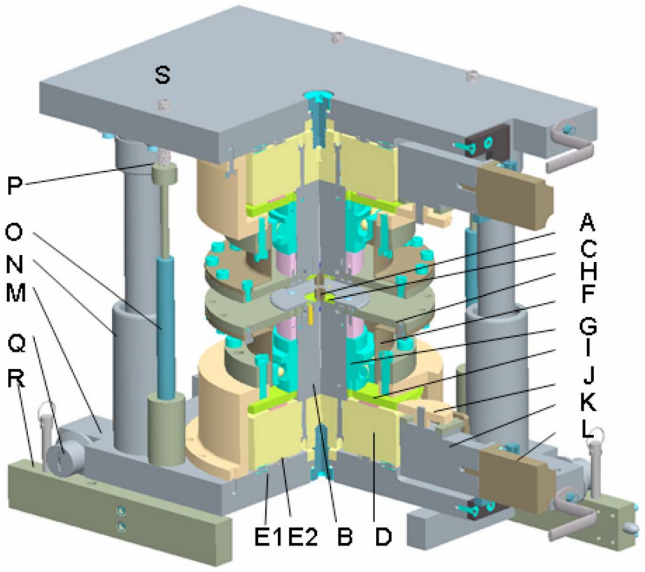

FIG. 3. (Color online) Cutaway view of the high pressure tomography apparatus. The sample is compressed by a pair of Drickamer anvils (A), supported by a steel column (B), through a WC spacer (C). The column is supported by a steel disk (D), to spread the load onto two concentric low-profile thrust bearings (E1 and E2) on each half of the apparatus. The load support column (B) and the Drickamer anvil are attached to the passive rotating member [flexspline (F)] of the HarmonicDrive™ unit, driven by the active member [wave generator; (G)] of the unit, through the coupler plate (H). The wave generator is attached to a large precision gear (I), driven by a smaller gear (J), through a right-angle gear box (K) and a stepper motor (L). The apparatus is mounted in a die set, with the thrust bearings loaded in the hardened steel die plate (M). The top and bottom halves of the apparatus are aligned by four ball-bearing die posts (N) and kept separated at a desired distance by four gas springs (O). The bottom die plate has rollers (Q) so that the entire apparatus can be rolled in and out of the hydraulic press over the transport rails (R). Screws (S) through the tapped holes in the top die plate allow the top half to be raised and lowered during loading and removal the Drickamer anvils containing a sample assembly.

anvils, and truncation size were determined empirically and are described in more detail elsewhere.[9] Depending on the truncation size and tapering angles of the anvils, we have successfully attained 8 GPa with a load of 25 T.

B. The load-bearing rotation mechanism

The rotational Drickamer-anvil high-pressure apparatus is illustrated in Fig. 3. The schematic diagram in Fig. 3 shows the location of the sample compressed by the pair of Drickamer anvils and supported by steel columns through WC spacers. The columns above and below the sample in turn are supported by steel disks that spread the load onto two concentric low-profile thrust bearings. The load support columns and the Drickamer anvil are attached to the passive rotating members or Flexspline of the HarmonicDrive™ units driven by the active member of the upper and lower units (wave generator) through coupler plates. The wave generators are attached to large precision gears driven by smaller gears through right-angle gear boxes and stepper motors.

The load-bearing frame was designed to support a maximum of ~50 T on the thrust bearings in order to achieve ~10 GPa sample pressure using 3 mm diam anvil truncation tips. This was achieved by introducing a pair of concentric low-profile needle roller bearings at the end of each Drickamer anvil to reduce rotational friction. This configuration differs from Ref. 5, which employed only a single set of bearings. Moreover, because the thrust bearings and drive train assemblies are installed at the ends of both Drickamer anvils, the entire cell can be rotated simultaneously. This is essential for tomography studies, but the apparatus can also be used in a differentiation mode by rotating the top and bottom anvils independently. An example of this mode of operation is shown below. The axial dynamic and static load specifications of our rotational Drickamer are 148 and 1020 kN, respectively, for the large thrust bearings, and 91 and 560 kN, respectively, for the smaller thrust bearings. With the specified grease for lubricant, the effective frictional coefficient is 0.05, and the calculated torque for rotation is 745 N M at a motor speed of 2000 rpm delivered through the HarmonicDrive™ unit.

The 203 mm (8 in.) diam gear attached to the wave generator has 260 teeth machined on the outer rim and is driven by a preloaded gear with 80 teeth. The right-angle gear box has a gear ratio of 10:1. Overall, a total gear reduction of 5200:1 is achieved, allowing low applied torque to rotate the apparatus under hydraulic load. The angular resolution is 0.0167° per stepper motor revolution, with 400 steps per revolution.

C. The imaging setup

The GSECARS standard CMT setup[6] is used for HPXTM imaging (see schematics Fig. 1). This system con-

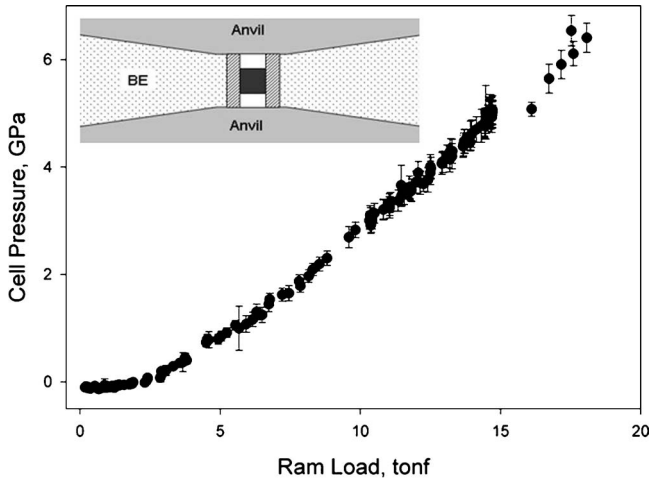

FIG. 4. An example of the pressure versus load calibrations for the Drickamer anvil cell used in the tomography test. The inset is a schematic of the cell assembly used in our tests. The sample is surrounded by a BN sleeve, with two end caps made of $Fe_{0.91}S_{0.01}$. Pressure medium is a mixture of boron and epoxy resin (BE).

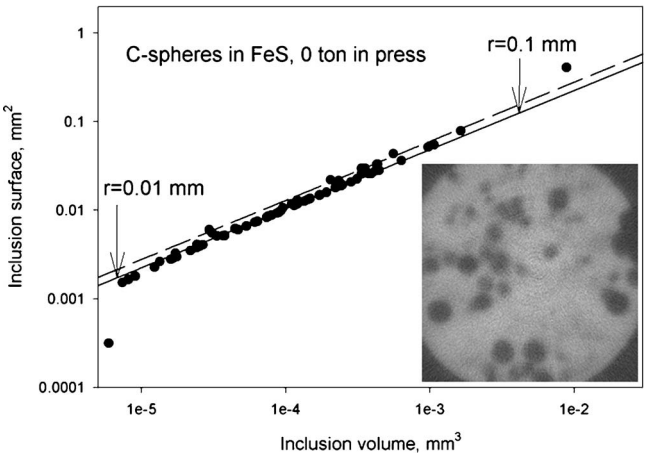

FIG. 5. Sphere surface area vs volume for the vitreous carbon spheres determined using the BLOB3D software package after 3D tomography reconstruction. Inset is an example of the tomography slices, where lighter material (C) is shown as a dark contrast. The sample diameter is 1 mm. The solid line is the relation for perfect spheres, dashed line for cubes. Note the deviation of the measurements from these theoretical relations below 4×10^{-6} mm^3 and above 5×10^{-3} mm^3. See text for discussion on spatial resolution evaluation.

sists of a Si (111) double-bounce monochromator, tunable to high photon energies (typically between 20 and 65 keV), a scintillator made of a YAG single crystal (about 30 mm diameter and 0.2 mm thick, optically polished) that converts transmitted x-ray contrast into visible light, and a 45° mirror that reflects the visible light signal into the objective lens, which then projects the image to the focal plane of the Roper MicroMax charge coupled device camera. Typical CMT operation procedure and data analysis software are given in Ref. 10.

IV. TEST RESULTS

A. Pressure generation and measurement

Prior to the system testing, a series of tests was conducted on pressure generation in the Drickamer cell, using various anvil geometries and containment ring materials. After extensive testing,[9] the optimum performance was found for a combination of 10 mm anvil diameter, 3 mm anvil tip diameter, 10° taper angle, with 5 mm wall thickness Al alloy rings. Figure 4 shows test results on pressure generation for this configuration. On increasing hydraulic load, the cell pressure (measured using NaCl diffraction lines based on the Decker equation of state[11]) increases almost linearly, reaching ~7 GPa at 20 tons. We use this pressure calibration in this study. Samples were shortened significantly during compression. Image analysis indicates that majority of the shortening occurred inside the sample assembly, so that the initially 2.5 mm long sample chamber became 1 mm at the peak load (see Fig. 4).

B. High pressure tomography tests

Two feasibility experiments were undertaken to test the operational features of our new high-pressure tomography system. The first experiment was designed to: (1) evaluate the resolution of high-pressure tomography in the Drickamer cell and (2) to examine the feasibility of performing shear deformation and tracking evolution of sample texture. The second test was to examine the feasibility of accurately measuring sample volume as a function of P and T by computed tomography. The sample for the first experiment consisted of vitreous carbon spheres ranging from 0.01 to 0.2 mm in diameter embedded in FeS powder, hot pressed at 1 GPa and 900 K. The sample for the second experiment consisted of a 0.8 mm diam sphere of vitreous Mg_2SiO_4 (v-Mg_2SiO_4) provided by J. Tangeman (Containerless Research, Inc.) and hot pressed in a FeS matrix at 1 GPa and 900 K. In both cases, the samples recovered from hot pressing were cylindrical in geometry with a diameter of 1 mm and length of 1 mm. Both the sample chamber (2 mm in height) and gaskets were made of a mixture of amorphous boron and epoxy resin. For test simplicity, no pressure marker was used in these tests; the pressures were estimated based on results from the pressure generation tests.

The monochromator was tuned to 35 keV, with collimated beam size of 2–3 mm. White field images were collected before and after the data collection by driving the HPXTM apparatus 3 mm horizontally, perpendicular to the incident beam. The distance was determined based on the size of the sample as well as the thickness of the Al containment ring, so that the white field image was not contaminated by the sample and, at the same time, remained completely within the "shadow" of the containment ring. At each pressure, a series of radiographs were taken, each for 10 s. The sample was rotated at either 0.25° or 0.5°, from 0° to 179.5° or 179.75°, respectively. The data were binned by 2×2 pixels, corresponding to 3.67 μm per pixel after binning.

1. Spatial resolution test

The first test of spatial resolution was performed at various hydraulic loads from 0 to 6 T, at 2 T increments. The sample contained a distribution of carbon spheres of different diameters. At a given pressure areas and volumes of the

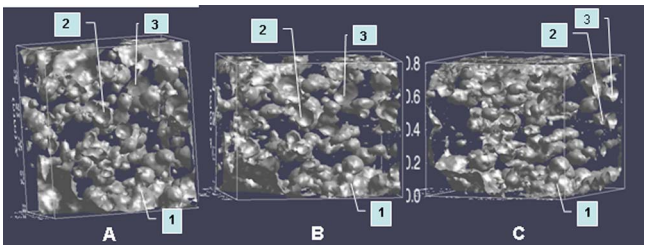

FIG. 6. (Color online) 3D images of the sample containing carbon spheres under three conditions: ambient (A), 6 T load (B), and 5 T load after shear by twisting the top and bottom Drickamer anvils by 180° (C). Spheres are represented as iso-intensity shells (and some are shown as partial spherical shells due to the cut in 3D imaging). A three-sphere chain (labeled as 1) can be seen near the bottom of each image. Two half spherical shells (labeled 2 and 3) are identified to guide the eye for examination of texture evolution. Note significant shortening of the sample after 6 T load (about 3 GPa), compared to the ambient sample. Also, note the pronounced shape change in the carbon spheres in (B): most spheres become ellipsoids with their long axes perpendicular to the loading axis. A comparison between (B) and (C) shows effects of shearing: spheres 2 and 3 have undergone a large angular displacement due to the twisting. It is thus possible to track inclusion locations and shape changes to obtain information on inclusion and matrix strain during deformation.

spheres were determined by tomography. The inset of Fig. 5 shows a representative slice from the tomographic reconstruction at 0 T within the high-pressure apparatus, before loading. Visual examination of individual slices indicated that features as small as 3–4 pixels can be recognized. Quantitative evaluation of spatial resolution is difficult. We examined the 3D reconstruction images using the BLOB3D software package (R.A. Ketcham, HRXCT Facility, University of Texas at Austin, Austin, TX, USA, unpublished data) and extracted volume and surface area information on the carbon spheres. Figure 5 plots sphere surface area versus volume, based on our BLOB3D extraction, inside the HPXTM but under ambient conditions. The data (solid circles) are compared with the relationship between surface area and volume for perfect spheres (solid line). Clearly, this relation holds well over a wide range of sphere sizes. However, at volumes below about 4×10^{-6} and above 5×10^{-3}, the measurements begin to deviate from the perfect sphere trend. The deviation at the low-volume end of the trend in Fig. 5 corresponds to a sphere radius of 0.01 mm, indicating a limit in spatial resolution of ~10 μm. The deviation at the high-volume end is likely due to the presence of large cracks and chippings near the corners of the hot-pressed sample. These are nearly 2D features, with higher surface-to-volume ratios.

To further evaluate the system imaging capabilities, we use the software package BLOB3D to analyze carbon sphere distribution as a function of hydraulic load. Figures 6(A) and 6(B) are two examples of extracted sphere distributions at 0 and 6 ton loads, respectively. The spheres can be tracked with increasing hydraulic load. Flattening of the sphere with increasing load is apparent in Fig. 6.

2. Shear deformation test

The sample tested in the above section was unloaded to 5 T, at which load the top and bottom Drickamer anvils were driven in opposite directions to introduce large shear strain to the sample. The sample was imaged when the top and bottom anvils were offset by 90° and 180°. Figure 6(C) shows the BLOB3D reconstruction of the spheres after 180° of shear rotation.

Comparing Figs. 6(B) and 6(C), it is evident that the sample underwent large shear strain. The arrows in the figures identify the individual spheres as strain markers. By analyzing the shape change in individual spheres and the center positions of the spheres, it will be possible to extract strain partitioning between the inclusions and the matrix from experiments of this type.

3. Volume measurement test

The sample containing v-Mg_2SiO_4 sphere was compressed up to 15 T, at an increment of 3 T. After each tomography reconstruction, we used BLOB3D to analyze the data. By defining the interface between the sphere and the matrix as the steepest slope in the intensity variation, volume changes of the v-Mg_2SiO_4 sphere were calculated as a function of pressure using utilities in the BLOB3D package. The diameter of the sphere computed from the tomographic reconstruction at ambient conditions was 802 μm, which is in excellent agreement with the diameter of 804 μm measured using an optical comparator prior to hot pressing. Figure 7 shows a series of reconstructed volumes for the v-Mg_2SiO_4 sphere up to 12 T. At 15 T, the large sample deformation caused slight overlap of the images between the sphere and the outer sample sleeve (BN). The sample volume had to be divided in order to separate the sleeve from the v-Mg_2SiO_4 sphere (and hence the sphere image is not shown in Fig. 7), although this procedure should not degrade volume measurements.

Figure 8 is a plot of the sphere volume as a function of cell pressure, which was based on separate calibration measurements shown in Fig. 4. As a result of lacking in-situ pressure measurements are large (about 0.3–0.4 GPa). Error estimate on the volume measurements was based on the uncertainty in identifying the cutoff intensity in defining the sphere-matrix interface. From Fig. 8, a clear change in volume versus pressure can be observed, thus justifying the technique as a useful tool in directly measuring volume changes of noncrystalline materials as a function of both pressure and temperature. Unlike crystalline materials, whose specific density can be evaluated using x-ray diffrac-

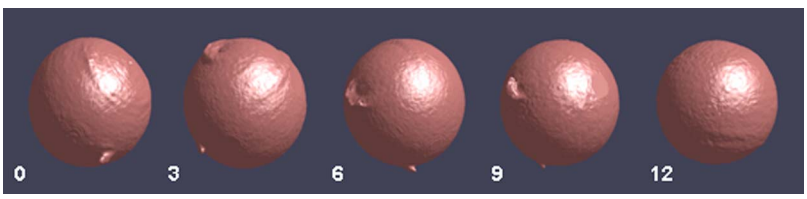

FIG. 7. (Color online) Examples of the vitreous Mg_2SiO_4 sphere images as a function of ram load in tons (labeled under each image). The image collected at 15 T is not shown because significant cell shortening caused the BN capsule to contact a small part of the sphere, and a special imaging dividing technique had to be applied.

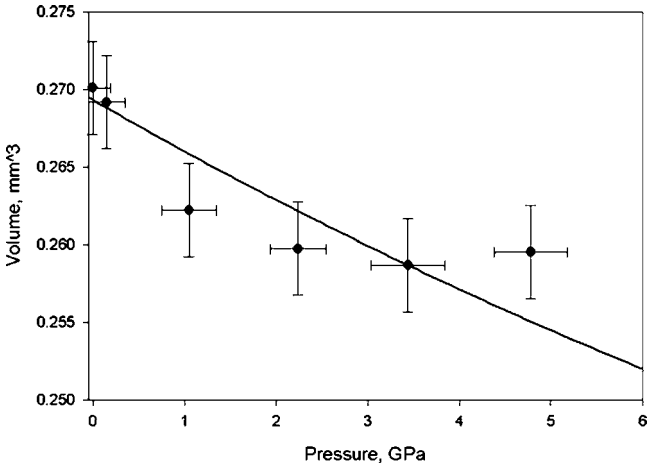

FIG. 8. A plot of the v-Mg_2SiO_4 sphere volume, determined using the extraction utility from BLOB3D, as a function of pressure. Pressures reported here are based on previous calibrations (Fig. 4) and are subject to large uncertainties (0.3–0.4 GPa). The fit using the second order Birch–Murnaghan equation of state (with $K'=4$) is shown as the solid curve. The actual volume decreases much faster at low pressures and then levels off, suggesting a strong pressure dependence in K'. Higher pressure data and more precise measurements are needed to determine the equation of state.

tion, densities of noncrystalline materials (glasses and melts) are traditionally more difficult to determine under high P and T. Our direct volume imaging technique provides a new method to address this long-standing difficulty. A fit to the data using the second order Birch–Murnaghan equation of state (with the pressure derivative of the bulk modulus K' fixed at 4) is shown as the solid curve. The actual volume decreases much faster at low pressures and then levels off, suggesting that K' for v-Mg_2SiO_4 varies with pressure.

V. DISCUSSION AND APPLICATIONS

We have shown that the new HPXTM is capable of recording tomographs under high pressure, currently with spatial resolutions of about 10 μm. Compared to conventional CMT, most of the resolution loss in high pressure CMT is primarily due to scattering of the high-energy photons required to penetrate through the pressure vessel. The technique is applicable to both crystalline and noncrystalline materials, but currently has limited resolving power in imaging materials with weak density/absorption contrasts, because of the high-energy photons used and the nonuniform attenuation of the pressure media. Other imaging techniques such as phase-contrast[12] and diffraction-enhanced[13] tomography may further improve imaging capabilities at high pressure in the future.

This technical development has enabled us to begin exploring applications in the following areas:

(1) Imaging microstructure evolution of composite materials under high pressure, temperature, and during deformation. Spatial distribution of constituent materials under varying physical conditions plays a critical role in controlling mechanical properties of the bulk composite. One of our major motives for the development of HPXTM is to study mechanisms of Fe-rich melts segregating from the silicate matrix. By performing melting experiments under high pressure and by quenching the sample at various stages of the melting process, the HPXTM will allow us to examine evolution of the Fe–silicate morphology. The information thus obtained will provide experimental constraint on formation scenarios of the Earth's core.

(2) Inclusions studies under pressure and temperature. By mimicking the geological conditions in the earth's deep interior at high P and T, it is possible to simulate inclusion formation history in the laboratory using this apparatus. Tomographs collected at various stages of the inclusion formation will help us understand the origin of nature inclusions found in minerals.

(3) Liquid properties. We have demonstrated the feasibility of measuring inclusion volumes by tomography imaging. This technique provides a direct means for glass and liquid volume measurement, allowing us to obtain information on equations of state of noncrystalline materials. The panoramic x-ray accessibility of the modified Drickamer cell also allows the determination of radial distribution function for liquids in the future using x-ray diffraction.

(4) Strain partitioning in composite materials. We have demonstrated that strains in the inclusions and the matrix can be determined by mapping the locations and shape change of the inclusions. This technique will be applied to silicate samples containing a certain volume fraction of Fe-rich melts. It is known that large shear can significantly alter the liquid connectivity network.[14] The combined shearing capability and tomography, with improved spatial resolution, will allow systematic experiments to be performed in this area.

(5) Neutron tomography. It is possible to apply a similar concept for a larger apparatus for high-pressure neutron tomography studies. Many problems related to light elements (e.g., hydrogen) and heavy elements (e.g., lanthanide metals) can be studied in greater detail using neutrons rather than x rays.

(6) It is also possible to replace the modified Drickamer cell with the diamond anvil cell for tomography studies to much higher pressures, although the reduction in sample volume may limit the usefulness of this technique.

ACKNOWLEDGMENTS

Work supported by NSF Grant No. EAR-0001088. The authors are grateful to valuable inputs and supports from S. Karato, D. Yamazaki, and I. Getting during the early stage of the development, and J. Tangeman (Containerless Research, Inc.) for providing vitreous Mg_2SiO_4 spheres for initial testing. We thank an anonymous reviewer for constructive comments. Work performed at GSECARS, Sector 13 of the Advanced Photon Source at Argonne National Laboratory. GSECARS is supported by the National Science Foundation—Earth Sciences, Department of Energy—Geosciences, W. M. Keck Foundation, and the U.S. Department of Agriculture. Use of the Advanced Photon Source was supported by the U.S. Department of Energy, Basic Energy Sciences, Office of Science, under Contract No. W-31-109-Eng-38.

[1] B. P. Flannery, H. Deckman, W. Roberge, and K. D'Amico, Science **237**, 1439 (1987).
[2] U. Bonse *et al.*, Nucl. Instrum. Methods Phys. Res. A **246**, 43 (1986).

[3] J. H. Kinney, S. R. Stock, M. C. Nichols, U. Bonse, and T. M. Breunig, J. Mater. Res. **5**, 1123 (1990).
[4] J. H. Kinney, D. L. Haupt, M. C. Nichols, T. M. Breunig, G. W. Marshall, Jr., and S. J. Marshall, Nucl. Instrum. Methods Phys. Res. A **347**, 480 (1994).
[5] D. Yamazaki and S. Karato, Rev. Sci. Instrum. **72**, 4207 (2001).
[6] M. L. Rivers, Y. Wang, and T. Uchida, Proc. SPIE **5535**, 783 (2004).
[7] Y. Wang *et al.*, Rev. Sci. Instrum. **72**, 2062 (2001).
[8] Y. Wang, M. Rivers, T. Uchida, P. Murray, G. Shen, S. Sutton, J. Chen, Y. Xu, and D. Weidner, in *Science and Technology of High Pressure, Proceedings of AIRAPT-17*, Honolulu, Hawaii, 25–30 July 1999, edited by M. H. Manghnani, W. J. Nellis, M. F. Nicols (Universities Press (India) Limited, Hyderabad, India, 2000), Vol. 2, pp. 1047–1052.
[9] T. Uchida, Y. Wang, F. Westferro, M. L. Rivers, J. Gebhardt, and S. R. Sutton, "X-ray microtomography under high pressure." Advances in High Pressure Mineralogy, Proceedings of the Geological Society of America, edited by E. Ohtani, submitted, 2005, Bloomington, Indiana.
[10] M. L. Rivers, S. R. Sutton, and P. Eng, Proc. SPIE **3772**, 78 (1999).
[11] D. L. Decker, J. Appl. Phys. **42**, 3239 (1971).
[12] P. Cloetens *et al.*, J. Phys. D **32**, A145 (1999).
[13] M. Ibison, K. C. Cheung, K. Siu, C. J. Hall, R. A. Lewis, A. Hufton, S. J. Wilkinson, K. D. Rogers, and A. Round, Nucl. Instrum. Methods Phys. Res. A (in press).
[14] D. Bruhn, N. Groebner, and D. L. Kohlstedt, Nature (London) **403**, 883 (2000).